Remote Sensing Letters
Publication details, including instructions for authors and subscription information:
http://www.tandfonline.com/loi/trsl20

Exploring the unusual uranium enrichment zones in the Thar Desert, India, using remote sensing, GIS and gamma-ray spectroscopy

Rishikesh Bharti[a] & D. Ramakrishnan[a]
[a] Department of Earth Sciences, Indian Institute of Technology Bombay, Mumbai, Maharashtra, India

Published online: 02 Jun 2015.

Remote Sensing Letters, 2015
Vol. 6, No. 7, 509–518, http://dx.doi.org/10.1080/2150704X.2015.1051629

Exploring the unusual uranium enrichment zones in the Thar Desert, India, using remote sensing, GIS and gamma-ray spectroscopy

Rishikesh Bharti and D. Ramakrishnan*

Department of Earth Sciences, Indian Institute of Technology Bombay, Mumbai, Maharashtra, India

(*Received 25 March 2015; accepted 8 May 2015*)

In this work, unusual enrichment of uranium and thorium in duricrusts associated with palaeochannels, palaeo alluvial plains and delta of the Thar Desert, India, is investigated. Optical and microwave satellite data, digital elevation model and 3D geographic information system were used to identify exposed, buried channels and associated duricrusts. It is evident from field radiometric surveys, geochemistry of soil and groundwater samples that zones of higher uranium (max 190 ppm) and thorium (max 142 ppm) concentration exist in the Thar. These enrichments are unusual and could be of economic significance.

1. Introduction

The recent discovery of near-surface secondary uranium deposits associated with palaeochannels and playas in Australia, South Africa and USA have received the attention of geoscientists from exploration perspectives (Carlisle 1978; Hambleton-Jones, Heard, and Toen 1984; Mann and Deutscher 1978; Arakel 1988; Hartleb 1988; Hou et al. 2007; Bowell et al. 2008; Noble, Gray, and Reid 2011). High concentration of radioactive minerals occurrence reported in these deposits is mainly confined to the palaeochannel systems (Hou et al. 2007). Source rocks, arid to semi-arid climate, geochemical transporting agents, evaporation, geochemical barriers, and suitable physical chemical conditions for precipitation are important factors which control secondary uranium enrichment in calcite (calcrete)-dominated and gypsum (gypcrete)-dominated duricrusts (Carlisle 1983; Arakel 1988; Bowell et al. 2008). These duricrusts can be easily mapped from hyperspectral as well as multispectral data using various processing techniques such as band ratio (Crosta and Mc. Moore 1989; Tangestani and Moore 2000; Ranjbar, Honarmand, and Moezifar 2004), linear mixture modelling (Bryant 1996), data fusion with decorrelation stretching (Kavak 2005) and spectral analysis (Crowley 1993; Ramakrishnan et al. 2013; Bharti and Ramakrishnan 2014). The aim of this article is to evaluate the potential of secondary uranium enrichments in parts of Thar Desert, India, using multispectral and hyperspectral remote sensing in conjunction with γ-ray spectrometry, fluorimetry and conventional geochemical approaches.

2. Study area

The study area is bounded by latitudes 24°–29° N and longitudes 70°–76° E covering the northern part of Gujarat and western part of Rajasthan, India. From source rock

*Corresponding author. Email: ramakrish@iitb.ac.in

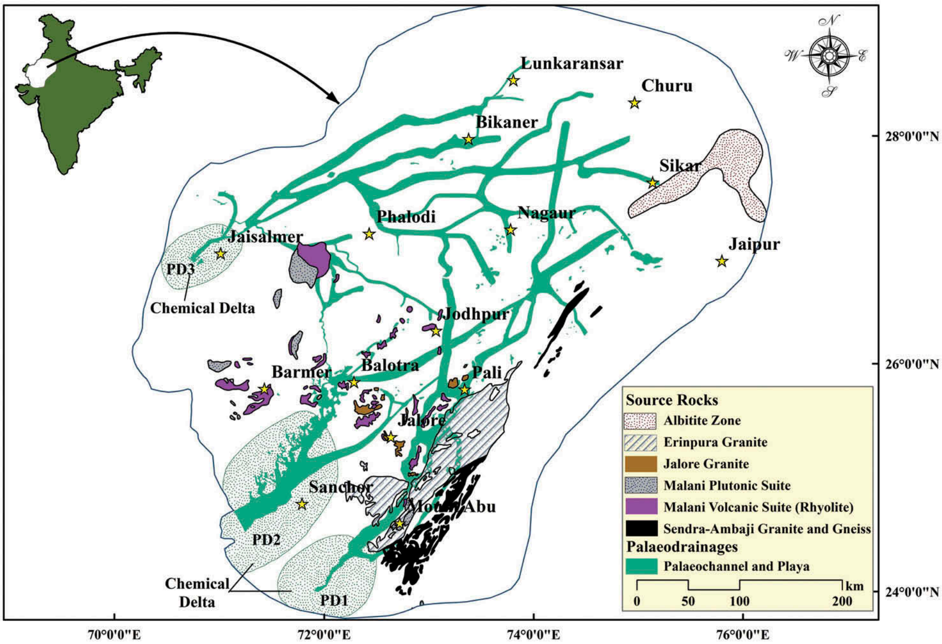

Figure 1. Map showing distribution of source rocks, palaeochannels, palaeodeltas and sampling sites.

perspectives, the investigated area has wide distribution of granites, rhyolites and albitite (Figure 1). These rocks have uranium (U), thorium (Th), vanadium (V) and potassium (K) in reasonable quantities (about 5 ppm). Fluvial and lacustrine deposits of Neogene and early Quaternary periods of the Thar Desert testifies extensive weathering and well-knitted palaeodrainage system that has the potential of flushing the soluble salts from the source rocks. These flushed salts are precipitated along the palaeochannels and Palaeo Deltas (PD) where the redox potential of the solution changes. The onset of aridity since the Holocene period accentuated the evaporative concentration of salts and their precipitation (Sinha, Stueben, and Berner 2004). Considering the source rocks, processes and changes in climatic regimes, the study area offers scope for potential secondary uranium enrichment.

3. Methodology

The methodology adopted in this study includes (i) delineation of palaeochannel courses using Radarsat-1, Landsat Enhanced Thematic Mapper Plus (ETM+) data and Shuttle Radar Topography Mission (SRTM) Digital Elevation Model (DEM), (ii) analysis of Hyperion data for mapping the spatial distribution of duricrusts, (iii) field radiometry and collection of duricrust and groundwater samples for analyses and (iv) geochemical analyses to estimate the concentration of radioactive elements. From the raw data of Radarsat-1, multilook images were derived and subsequently enhanced using Lee-Sigma filter for delineating surface and near-surface drainage patterns following the procedures of Ghoneim and El-Baz (2007). In addition to Radarsat-1 data, Landsat-7 ETM+ optical data were also used. The channels delineated from the Radarsat-1 and ETM+ were subsequently laid over the SRTM DEM using 3D geographic information system (GIS) to validate the flow gradient. For this purpose, topographic profiles (elevation versus distance) were constructed at several transects (along and across the piedmont slope) to identify the channel cross sections and their gradients.

For mapping the duricrusts, Hyperion data were used. Out of 242 bands, calibrated and noise-free 158 spectral bands were subjected to atmospheric correction (Adler-Golden et al. 1999) using Fast Line-of-Sight Atmospheric Analysis of Spectral Hypercubes (FLAASH) module of Environment for Visualization software. Noise reduction of visible, near-infrared and shortwave infrared bands was achieved independently by using minimum noise fraction (Green et al. 1988) algorithm. Finally, Spectral Angle Mapper (SAM) technique (Equation (1); Kruse et al. 1993) was used to map the spatial distribution of calcrete and gypcrete by measuring the similarity between the reference (measured calcrete spectra) and unknown (pixel) spectra.

$$\alpha = \cos^{-1}\left[\frac{\sum_{i=1}^{n} t_i r_i}{\left(\sum_{i=1}^{n} t_i^2\right)^{1/2}\left(\sum_{i=1}^{n} r_i^2\right)^{1/2}}\right] \tag{1}$$

where t_i is the target spectrum (image), r_i is the reference spectrum (library), i is the number of input spectral bands (1, 2, 3, …, n) and α is the angle between target and reference spectrum.

By overlaying the palaeochannel and duricrust layers in GIS, potential sites of valley calcrete/gypcrete were identified. Subsequently, field radiometric survey was carried out in these areas using γ-ray spectrometer (Radiations Solutions 230 Bismuth Germanium Oxide detector). This calibrated equipment can be directly employed in the field to estimate the concentrations of K (%), U (ppm) and Th (ppm). Calcrete, gypcrete and groundwater samples were also collected from the anomalous areas (identified through γ-ray spectrometer) for further geochemical analyses. For uranium analysis, pH of water samples was maintained below 2 using nitric acid to prevent it from biological activities and precipitation (Tosheva, Stoyanova, and Nikolchev 2004; Waterwatch 2005; Jobbágy et al. 2009; Kumar et al. 2011).

4. Results and discussions

The distribution of palaeochannels and playas was mapped by overlaying ETM+ colour composite (blue:band 7, green: principal component 1 and red:band 4) and processed Radarsat-1 data on DEM. It is evident from Figure 1 that drainage network of the investigated area belongs to three different trends and ages (Roy and Jakhar 2001). This includes (i) the oldest NNE–SSW trending drainage system running parallel to the Aravalli mountain front and draining its waters to Little Rann of Kutch; (ii) the older, westerly flowing drainage network along the piedmont slope of the Aravalli mountains and draining its waters to Indus and, finally, (iii) the palaeo and present Luni river system with a NE–SW trend, which drains into the Great Rann of Kutch. Accordingly, three different migration pathways and areas of chemical deltas were identified (PD1–PD3). These chemical deltas are distributed around Little Rann of Kutch (PD1), Jaisalmer area (PD2) with several active and dry playas, and the zone developed by the present and palaeo Luni river system adjoining the Great Rann of Kutch (PD3). It is interesting to note that several of the prevailing and defunct playas are aligned along these palaeodrainage paths and appear to have evolved due to blocking of river systems.

Though U has characteristic reflectance spectral absorption features in the visible region, it is often difficult to identify their presence based on this due to low concentration (usually in ppm). However, in pheritic environment, U^{6+} species co-precipitate with Mg-calcite and dolomite (Bharti and Ramakrishnan 2014; Gabitov et al. 2008; Nash 1981), which can be effectively exploited to identify and map the potential zones. Since scatter plot between MgO and U content of calcretes of the investigated area has high correlation (R^2 = 0.82, Figure 2), the Mg-calcrete was considered as a proxy for uranium mapping. Accordingly, the prominent Mg-calcite absorption feature occurring between 2.30 and 2.35 μm wavelength (Figure 3) was used to map the groundwater calcrete using Hyperion data. As the magnesium (Mg) content increases in calcrete, the 2.35 μm absorption feature shifts to 2.30 μm wavelength (Hunt and Salisbury 1970; Clark 1999; Christensen et al. 2000; Van-der-Meer 2004; Bharti and Ramakrishnan 2014). Based on this fact, representative lab-measured spectra of Mg-calcrete, processed Hyperion data and SAM technique were used to map the spatial distribution of Mg-calcrete (Figure 4) with 72.15% overall accuracy.

Table 1 depicts the concentration of radionuclides (U, Th and K) and major oxide chemistry. The values of uranium, thorium and potassium measured in the field ranges from 0.9 to 8.0 ppm, 0.9 to 35.0 ppm and 0.5 to 18.0%, respectively. Misra et al. (2011) have reported significantly higher uranium concentration in calcrete samples ranging from 13.5 ppm to 190.0 ppm from deep borehole samples in this area. The uranium concentration in water samples collected in this work

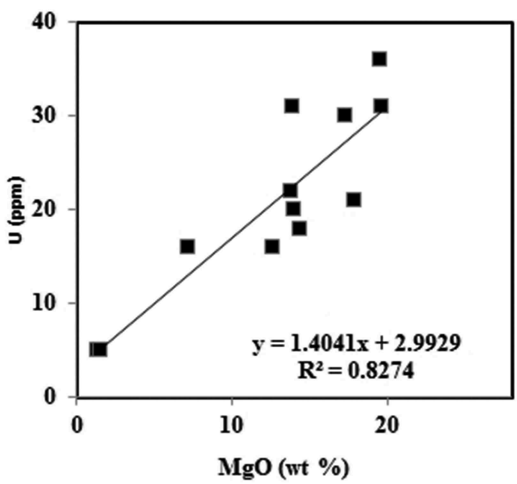

Figure 2. Scatter plots showing the strong, positive correlation between magnesium and uranium content of calcretes.

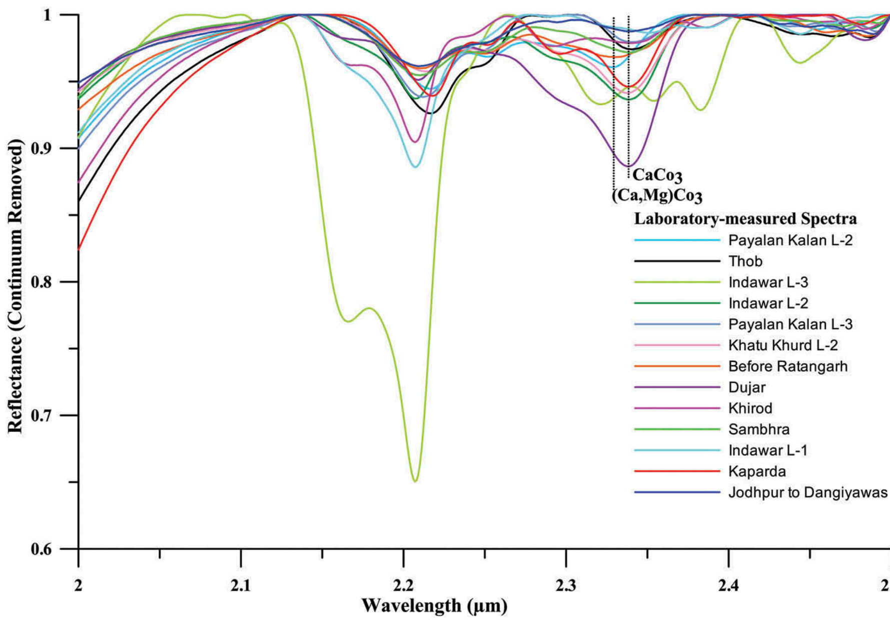

Figure 3. Characteristic spectral absorption features of some of the Mg-calcretes of the investigated area.

varies between 0.2×10^{-3} and 1791.7×10^{-3} mg l^{-1} (Table 2). From the spatial distribution of anomalous concentrations (20×10^{-3}–1791.7×10^{-3} mg l^{-1}) it is evident that such zones are typically located very close to the confluence of palaeochannels and deltas.

In the investigated area, source rocks of U, V and K such as albitite, Erinpura-, Malani-and Jalore-granite (Figure 1) are abundant (Kochhar 1989; GSI 1999, 2011). In addition to this, palaeo climate favoured intense weathering (Sinha, Stueben, and Berner 2004; Ramakrishnan and Tiwari 2006) of the above-mentioned source rocks and availability of well-knitted palaeochannel systems (Bajpai 2004; Jain, Tandon, and Bhatt 2004) to carry the U, V and K, supported the secondary uranium enrichments. The Thar Desert thereby satisfies all necessary conditions for secondary uranium enrichment in duricrusts associated with chemical deltas and palaeochannels. Thus mapping the distribution of duricrusts along the palaeochannels is an important component for exploring such deposits. The optical and microwave remote sensing data in conjunction with DEM is observed to be very efficient in delineating the palaeochannels and playas. The 3D GIS is particularly useful in perceiving the overall gradient changes and hence to identify the buried channels in pockets with high dunal cover. Hyperion data with 10 nm bandwidth is found to be very efficient in discriminating the Mg-calcretes from non-Mg-calcretes. This aspect is very vital in delineating the groundwater calcretes from other pedogenic calcretes of lesser importance.

It is evident from the field radiometric surveys that anomalous concentrations of U and Th exist in the duricrusts and groundwater samples. Prevalence of zones with very high concentrations of uranium (up to 190 ppm) associated with palaeochannels and playas

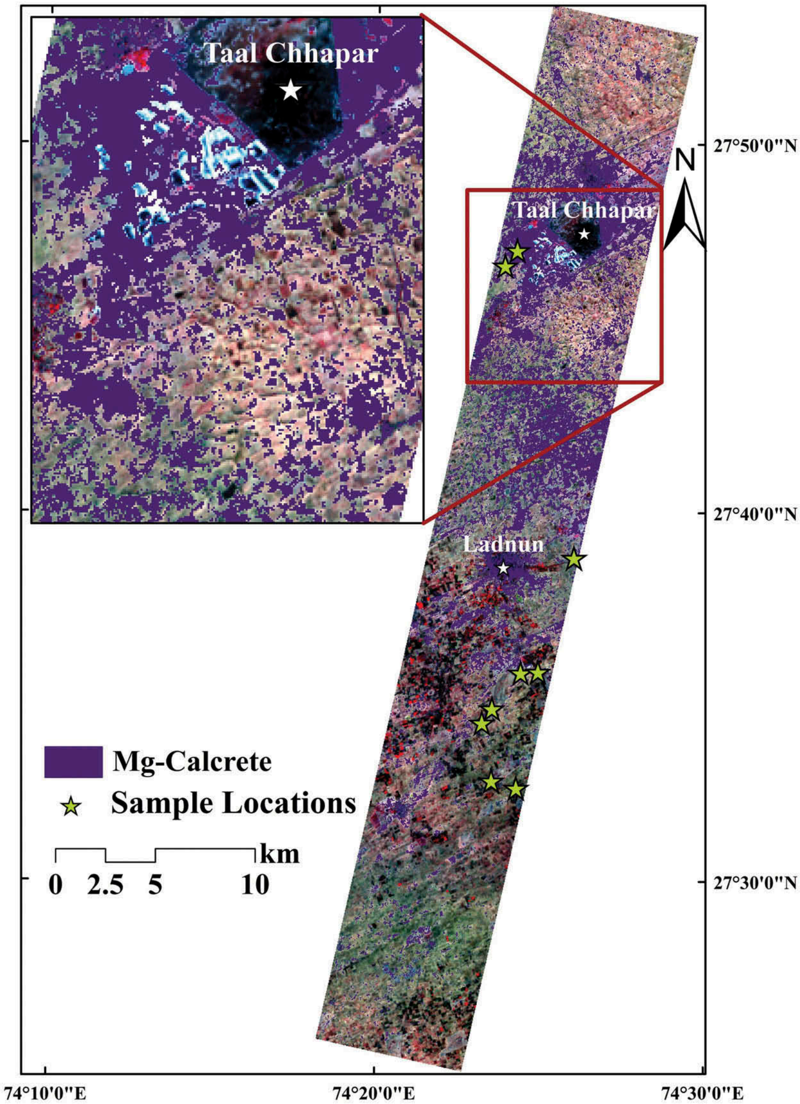

Figure 4. Results of SAM classification depicting distribution of Mg-calcretes. In the background, FCC of Hyperion (red: 0.72 μm; green: 0.58 μm; blue: 0.48 μm) is displayed.

certainly indicate their enrichment in secondary environment. Presence of very high concentration of uranium (21.9×10^{-3}–1791.7×10^{-3} mg l^{-1}) in groundwater also points to such enrichment process. These values are remarkably higher than the reported values of (1×10^{-3}–700×10^{-3} mg l^{-1}, with 14×10^{-3} mg l^{-1} mean value) Northern Yilgarn deposit (Noble, Gray, and Reid 2011). To sum up, this work mainly showcases the potential of adopted methodology involving optical and microwave remote sensing, γ-ray spectrometry and geochemical techniques in exploration of such unusual occurrences of uranium enrichment.

Table 1. Concentration of radionuclides and major oxides in the duricrusts.

	In situ values			Major oxide chemistry (percentage weight)							
Location name	U (ppm)	Th (ppm)	K (%)	CaO	Fe_2O_3	K_2O	MgO	P_2O_5	SiO_2	Al_2O_3	Na_2O_3
Indawar-1	2.2	1.4	11.8	4.8	9.5	3.0	3.3	0.1	48.3	30.3	0.6
Indawar-2	2.2	0.9	17.7	50.4	1.9	1.4	1.1	0.0	38.5	6.5	0.3
Indawar-3	8.0	30.7	8.0	15.4	4.0	0.7	0.8	0.0	48.1	30.9	0.2
Paylan Kalan-2	3.6	12.9	1.5	14.1	4.6	1.7	18.0	0.0	50.1	11.0	0.4
Paylan Kalan-3	3.6	12.9	1.5	21.5	5.2	2.0	4.3	0.1	54.2	12.4	0.3
Khirod	1.5	3.6	12.0	31.1	6.5	3.1	2.1	0.0	43.3	13.7	0.2
Thob	4.0	15.6	18.0	16.6	6.1	2.1	8.5	0.2	52.9	13.0	0.7
Ratangarh	4.0	14.0	2.1	26.7	4.2	1.8	13.8	0.1	45.0	7.8	0.6
Ranasar Beekan	5.0	20.0	2.0	36.8	3.1	1.3	13.0	0.1	39.0	6.0	0.8
Sambhra Playa	1.6	10.2	17.0	5.4	5.7	2.3	4.0	0.2	68.8	12.9	0.8
Kaparda	46.9	–	–	47.5	2.8	0.5	2.9	0.04	38.4	6.8	1.1
Jodhpur to Dangiyawas	43.2	–	–	4.7	5.7	3.8	2.9	0.07	63.3	18.3	1.2
Dujar	11.4	61.0	0.5	74.4	0.7	0.5	1.3	0.02	18.5	4.4	0.2
Malawas	43.2	142.3	2.0	66.6	0.8	1.4	1.5	0.04	25.0	4.4	0.4
Khatu Khurd-2	61.7	–	–	3.1	2.4	0.4	2.6	0.04	82.9	8.0	0.6
Didwana*	190	–	–	–	–	–	–	–	–	–	–
Charan Ka Bas*	49.5	–	–	–	–	–	–	–	–	–	–
Lachhiri*	13.5	–	–	–	–	–	–	–	–	–	–

Note: *After Misra et al. (2011).

Table 2. Concentration of uranium in groundwater samples.

Location name	U ($\times10^{-3}$ mg l^{-1})	Location name	U ($\times10^{-3}$ mg l^{-1})
Sardarshahar	12.2 ± 0.9	Bengti Kalan and Kundal	2.1 ± 0.4
Lunkaransar	4.1 ± 0.6	Near Gomat	12.4 ± 1.0
Aajdoli	112.8 ± 2.9	Rajpura	10.8 ± 0.6
Haryasar	21.9 ± 3.1	Gelawas	503.0 ± 61.4
Mankeria	18.8 ± 1.2	Sev ki Galan	445.0 ± 41.1
Churu	42.7 ± 2.2	Mokalsar	3.9 ± 0.5
Dandalwas	7.8 ± 0.7	Munthala Kaba-1	216.8 ± 35.6
Deriya	45.9 ± 2.9	Munthala Kaba-2	401.6 ± 52.8
Indawar	0.8 ± 0.3	Aampura	50.1 ± 15.9
Bagar	7.2 ± 1.6	Tharad	1508.2 ± 126.9
Dadawadi Temple	0.2 ± 0.1	Matasukh	1791.7 ± 159.6
Hadda Village	2.0 ± 0.5	Kotarwada	920 ± 56.2
Ladnun to Didwana	16.7 ± 1.8	Sikhar	0.5 ± 0.1
Ber Village	11.5 ± 0.7	Sopra Village	5.5 ± 0.5
Ber Village	11.0 ± 1.9	Khatu Khurd	10.2 ± 0.9
Jhardiya	7.2 ± 0.8	Thob Gypsum Mine	71.9 ± 5.8
Kishanpura	12.2 ± 1.3	Malawas	6.8 ± 0.7
Jalore	81.9 ± 20.3	Dujar Village	21.9 ± 1.9
Doongri	1.5 ± 0.3	Somaser	20.7 ± 1.8
Bhukan-1	20.0 ± 4.9	Parihara	13.8 ± 1.6
Bhukan-2	38.3 ± 3.9	Chandan	18.8 ± 1.7

Disclosure statement

No potential conflict of interest was reported by the authors.

Funding

This work was supported by the Indian Space Research Organization (ISRO), Government of India, India [grant number 12ISROC006].

References

Adler-Golden, S. M., M. W. Matthew, L. S. Bernstein, R. Y. Levine, A. Berk, S. C. Richtsmeier, P. K. Acharya, et al. 1999. "Atmospheric Correction for Short-Wave Spectral Imagery Based on MODTRAN4." *Proceedings SPIE* 3753: 61–69.

Arakel, A. V. 1988. "Carnotite Mineralization in Inland Drainage Areas of Australia." *Ore Geology Reviews* 3 (1–3): 289–311. doi:10.1016/0169-1368(88)90023-6.

Bajpai, V. N. 2004. "Hydrogeological Evolution of the Luni River Basin, Rajasthan, Western India: A Review." *Proceedings of the Indian Academy of Sciences- Earth and Planetary Sciences* 113 (3): 427–451.

Bharti, R., and D. Ramakrishnan. 2014. "Uraniferous Calcrete Mapping Using Hyperspectral Remote Sensing." In *IEEE International Geoscience and Remote Sensing Symposium (IGARSS)*, Quebec City, QC, July 13–18, 2902–2905. doi:10.1109/IGARSS.2014.6947083.

Bowell, R. J., M. Booysens, A. Pedley, J. Church, and A. Moran. 2008. "Characterization of Carnotite Uranium Deposit in Calcrete Channels, Trekkopje, Namibia." Proceedings of Africa Uncovered: Mineral Resources for the future, SEG-GSSA Conference, Misty Hills, July 7–10, 114–121.

Bryant, R. G. 1996. "Validated Linear Mixture Modelling of Landsat TM Data for Mapping Evaporite Minerals on a Playa Surface: Methods and Applications." *International Journal of Remote Sensing* 17 (2): 315–330. doi:10.1080/01431169608949008.

Carlisle, D. 1978. *The Distribution of Calcretes and Gypcretes in the Southwestern United States and Their Uranium Favourability*. Grand Junction, Dept. Energy Report, Open File Report, University of California, Los Angeles, GJBX-29(78), 1–274.

Carlisle, D. 1983. "Concentration of Uranium and Vanadium in Calcretes and Gypcretes." *Geological Society, London, Special Publications* 11: 185–195. doi:10.1144/GSL.SP.1983.011.01.19.

Christensen, P. R., J. L. Bandfield, V. E. Hamilton, D. A. Howard, M. D. Lane, J. L. Piatek, S. W. Ruff, and W. L. Stefanov. 2000. "A Thermal Emission Spectral Library of Rock-Forming Minerals." *Journal of Geophysical Research (Planets)* 105 (E4): 9735–9739.

Clark, R. N. 1999. "Spectroscopy of Rocks and Minerals, and Principles of Spectroscopy." In *Manual of Remote Sensing, Remote sensing for the Earth Sciences*, edited by A. N. Renez, Vol. 3, 3–58. New York: John Wiley and Sons.

Crosta, A., and J. M. Mc.Moore. 1989. "Enhancement of Landsat Thematic Mapper Imagery for Residual Soil Mapping in SW Minais Gerais State, Brazil: A Prospecting Case History in Greenstone Belt Terrain." In *International Proceedings of the Seventh Erim Thematic Conference: Remote Sensing for Exploration Geology*, Calgary, Alberta, Canada, 2–6 October, 1173–1187.

Crowley, J. K. 1993. "Mapping Playa Evaporite Minerals with AVIRIS Data: A First Report from Death Valley, California." *Remote Sensing of Environment* 44 (2–3): 337–356. doi:10.1016/0034-4257(93)90025-S.

Gabitov, R. I., G. A. Gaetani, E. B. Watson, A. L. Cohen, and H. L. Ehrlich. 2008. "Experimental Determination of Growth Rate Effect on U^{6+} and Mg^{2+} Partitioning between Aragonite and Fluid at Elevated U^{6+} Concentration." *Geochimica Et Cosmochimica Acta* 72: 4058–4068. doi:10.1016/j.gca.2008.05.047.

Ghoneim, E., and F. El-Baz. 2007. "Dem-Optical-Radar Data Integration for Palaeo-Hydrological Mapping in the Northern Darfur, Sudan: Implication for Groundwater Exploration." *International Journal of Remote Sensing* 28 (22): 5001–5018. doi:10.1080/01431160701266818.

Green, A. A., M. Berman, P. Switzer, and M. D. Craig. 1988. "A Transformation for Ordering Multispectral Data in Terms of Image Quality with Implications for Noise Removal." *IEEE Transactions on Geoscience and Remote Sensing* 26: 65–74. doi:10.1109/36.3001.

GSI. 1999. *Geological and Mineral Map of Rajasthan*. *Geological Survey of India*. Government of India, India.

GSI. 2011. *Geology and Mineral Resources of Rajasthan*, 131 p. Geological Survey of India. Miscellaneous Publication No. 30 Part 12. 3rd rev. ed. Jaipur: Geological Survey of India.

Hambleton-Jones, B. B., R. G. Heard, and P. D. Toen. 1984. "Exploration for Surficial Uranium Deposits." In *Surficial Uranium Deposits*, edited by P. D. Toen, 61–64. Vienna: IAEA-Tecdoc-322.

Hartleb, J. W. O. 1988. "The Langer Heinrich Uranium Deposit: Southwest Africa/Namibia." *Ore Geology Reviews* 3: 277–287. doi:10.1016/0169-1368(88)90022-4.

Hou, B., A. J. Fabris, J. L. Keeling, and M. C. Fairclough. 2007. "Cainozoic Palaeochannels Hosted Uranium and Current Exploration Methods, South Australia." *MESA Journal* 46: 34–39.

Hunt, G. R., and J. W. Salisbury. 1970. "Visible and near Infrared Spectra of Minerals and Rocks: I Silicate Minerals." *Modern Geology* 1: 283–300.

Jain, M., S. K. Tandon, and S. C. Bhatt. 2004. "Late Quaternary Stratigraphic Development in the Lower Luni, Mahi and Sabarmati River Basins, Western India." *Proceedings of the Indian Academy of Sciences- Earth and Planetary Sciences* 113 (3): 453–471.

Jobbágy, V., I. Chmielewska, T. Kovács, and S. Chałupnik. 2009. "Uranium Determination in Water Samples with Elevated Salinity from Southern Poland by Micro Coprecipitation Using Alpha Spectrometry." *Microchemical Journal* 93: 200–205. doi:10.1016/j.microc.2009.07.006.

Kavak, K. S. 2005. "Recognition of Gypsum Geohorizons in the Sivas Basin (Turkey) Using ASTER and Landsat ETM+ Images." *International Journal of Remote Sensing* 26 (20): 4583–4596. doi:10.1080/01431160500185607.

Kochhar, N. 1989. "High Heat Producing Granites of the Malani Igneous Suite, Northern Peninsular India." *Indian Minerals* 43: 339–346.

Kruse, F. A., A. B. Lefkoff, J. W. Boardman, K. B. Heidebrecht, A. T. Shapiro, P. J. Barloon, and A. F. H. Goetz. 1993. "The Spectral Image Processing System (Sips)—Interactive Visualization and Analysis of Imaging Spectrometer Data." *Remote Sensing of Environment* 44: 145–163. doi:10.1016/0034-4257(93)90013-N.

Kumar, A., S. Rout, U. Narayanan, M. K. Mishra, R. M. Tripathi, J. Singh, S. Kumar, and H. S. Kushwaha. 2011. "Geochemical Modelling of Uranium Speciation in the Subsurface Aquatic Environment of Punjab State in India." *Journal of Geology and Mining Research* 3 (5): 137–146.

Mann, A. W., and R. L. Deutscher. 1978. "Genesis Principles for the Precipitation of Carnotite in Calcrete Drainages in Western Australia." *Economic Geology* 73: 1724–1737. doi:10.2113/gsecongeo.73.8.1724.

Misra, A., D. Pande, K. R. Kumar, L. K. Nanda, P. B. Maithani, and A. Chaki. 2011. "Calcrete-Hosted Surficial Uranium Occurrence in Playa-Lake Environment at Lachhri, Nagaur District, Rajasthan, India." *Current Science* 101 (1): 84–88.

Nash, J. T. 1981. "Geology of Dolomite-Hosted Uranium Deposits at the Pitch Mine, Saguache County, Colorado." In *Western Slope Colorado, New Mexico Geological Society Guidebook, Field Conference*, Vol. 32, edited by R. C. Epis and J. F. Callender, Socorro, October 8–10, 191–198. The Society.

Noble, R. R. P., D. J. Gray, and N. Reid. 2011. "Regional Exploration for Channel and Playa Uranium Deposits in Western Australia Using Groundwater." *Applied Geochemistry* 26 (12): 1956–1974. doi:10.1016/j.apgeochem.2011.06.027.

Ramakrishnan, D., M. Nithya, K. D. Singh, and R. Bharti. 2013. "A Field Technique for Rapid Lithological Discrimination and Ore Mineral Identification: Results from Mamandur Polymetal Deposit, India." *Journal of Earth System Sciences* 122 (1): 93–106. doi:10.1007/s12040-012-0255-x.

Ramakrishnan, D., and K. C. Tiwari. 2006. "Calcretized-Ferricretes Around Jaisalmer Area, Thar Desert, India: Their Chemistry, Mineralogy, Micromorphology and Genesis." *Turkish Journal of Earth Science* 15 (2): 1–13.

Ranjbar, H., M. Honarmand, and Z. Moezifar. 2004. "Application of the Crosta Technique for Porphyry Copper Alteration Mapping, Using ETM+ Data in the Southern Part of the Iranian

Volcanic Sedimentary Belt." *Journal of Asian Earth Sciences* 24: 237–243. doi:10.1016/j.jseaes.2003.11.001.

Roy, A. B., and S. R. Jakhar. 2001. "Late Quaternary Drainage Disorganization, and Migration and Extinction of Vedic Saraswati." *Current Science* 81 (9): 1188–1195.

Sinha, R., D. Stueben, and Z. Berner. 2004. "Palaeohydrology of the Sambhar Playa, Thar Desert, India, Using Geomorphological and Sedimentological Evidences." *Journal Geological Society of India* 64: 419–430.

Tangestani, M. H., and F. Moore. 2000. "Iron Oxide and Hydroxyl Enhancement Using the Crosta Method: A Case Study from the Zagros Belt, Fars Province, Iran." *International Journal of Applied Earth Observation and Geoinformation* 2 (2): 140–146. doi:10.1016/S0303-2434(00)85007-2.

Tosheva, Z., K. Stoyanova, and L. Nikolchev. 2004. "Comparison of Different Methods for Uranium Determination in Water." *Journal of Environmental Radioactivity* 72: 47–55. doi:10.1016/S0265-931X(03)00185-1.

Van-der-Meer, F. 2004. "Analysis of Spectral Absorption Features in Hyperspectral Imagery." *International Journal of Applied Earth Observation and Geoinformation* 5: 55–68. doi:10.1016/j.jag.2003.09.001.

Waterwatch. 2005. *Australia National Technical Manual. Module-6 Groundwater Monitoring*. Canberra: Department of the Environment and Heritage.